137. Conjugative, Exciton and Charge-Resonance Interactions in D_{2d}-9,9'-Spirobifluorene and D_{2d}-Tetrabenzotricyclo[5.5.0.$0^{2,8}$]dodeca-3,5,9,11-tetraene. Photoelectron and Polarized Absorption Spectra

by **Jens Spanget-Larsen, Rolf Gleiter** and **Rudolf Haider**

Institut für Organische Chemie der Universität Heidelberg, D-6900 Heidelberg

(29.III.83)

Summary

Photoelectron spectroscopy, polarized electronic absorption spectroscopy in stretched polymer sheets, and semiempirical theoretical methods have been applied to investigate the valence electronic structures of the two title compounds **1** and **2**, considering fluorene (**3**) as a reference compound. The results are analyzed in terms of 'through space' and 'through bond' conjugative effects and exciton and charge-resonance interactions. Spiro-conjugation in **1** is found to play a similar role as 'through bond' interaction *via* the cyclobutane ring in **2**. In contrast to the results of a recent investigation, exciton coupling is found to be relatively insignificant, while charge-resonance effects are important. The transition close to 41000 cm^{-1} in the absorption spectra of **1** and **2** has no obvious counterpart in the spectrum of **3**; it is assigned to a $^1E^-$ state with large charge-resonance character, involving promotion of an electron from the HOMO of one half-chromophore to the LUMO of the other.

1. Introduction. – Recently we proposed that in tricyclic π-systems of the type **B** the four-membered ring should act like a relay, enabling the two π-moieties to interact 'through bond' [1]. The magnitude of this interaction should be comparable to that of the corresponding spiro-type 'through space' interaction [2] in the case

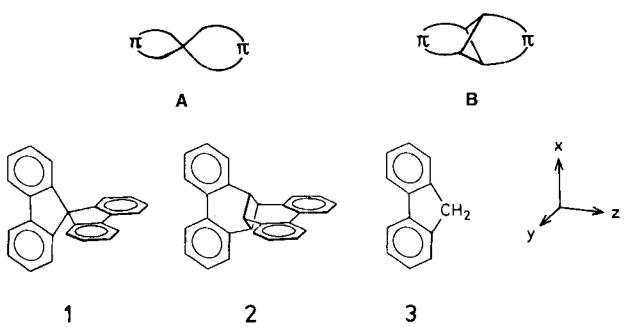

of **A**. Models to test this proposal are 9,9′-spirobifluorene (**1**) and tetrabenzotricyclo[5.5.0.$0^{2,8}$]dodeca-3,5,9,11-tetraene (**2**, =8b,8c,16b,16c-tetrahydrocyclobuta-[1,3-1:2,4-1′]diphenanthrene). Furthermore, in close relation to the question of long-range conjugative interactions, **1** and **2** are interesting model compounds for the study of exciton and charge-resonance interactions between weakly coupled identical chromophores [3] [4]. In this paper we discuss all three effects in a detailed investigation of low-lying electronically excited states for **1** and **2**, thereby considering fluorene **3** as a suitable reference compound.

So far no detailed investigation of the electronic structure of **2** has been published, but fluorene **3** and spirobifluorene **1** have been the subject of several spectroscopic investigations. Comparison of the photoelectron (PE) spectra of **3** [5] [6] and **1** [7] provided the first unambigous demonstration of spiro-conjugation [2], as described by *Schweig et al.* [7]. The polarized absorption spectra of **3** and/or **1** have been studied by several authors, *e.g.* [8–12]. An extensive experimental investigation was carried out recently by *Sagiv et al.* [11] who measured the polarized absorption spectra of biphenyl, **1**, **3**, and '[6,6]vespirene' (a chiral alkyl derivative of **1**) in stretched polyethylene at room temperature. *Sagiv et al.* interpreted the spectra in terms of simple exciton theory [3] [4] and suggested a reassignment of part of the observed transitions.

The present investigation is based on polarized absorption spectroscopy in stretched polyethylene at 77 K. Our spectral analysis of **1** and **2** is based on correlation with the data for 'monomer' **3**, using a molecular orbital (MO) picture and supported by the results of PE spectroscopy and semi-empirical procedures. Our results are at variance with the conclusions of *Sagiv et al.* [11] in several essential points.

2. Experimental. – **2** was synthesized according to the method described by *Wittig & Skipka* [13] [14]. Samples of **1** and **3** were kindly provided by Prof. Dr. *D. Hellwinkel.* The He(Iα) gas-phase PE spectrum of **2** was recorded with the sample heated to a temperature of 510 K. At this temperature, cycloreversion of **2** may take place. The spectrum shown in *Figure 2* may thus be influenced by the presence of an olefinic impurity.

The linear dichroic (LD) absorption spectra of **1**, **2** and **3** in stretched polyethylene were measured at 77 K as described previously [15] [16], and reduced according to the 'TEM' stepwise reduction procedure of *Eggers et al.* [17–19].

3. Calculational Details. – Semi-empirical calculations were carried out using either the PPP [20] or the CNDO/S [21] formalism. In the PPP calculations the electron interaction integrals were estimated according to *Mataga & Nishimoto* [22] with a γ-value of 10.84 eV. All bond lengths were taken as 140 pm and the biphenyl fragments were assumed to possess local D_{2h}-symmetry; an overall D_{2d}-symmetry was assumed for **1** and **2**. Inductive and hyperconjugative effects of the saturated C-centers in **1** and **3** were neglected. 'Through space' spiro-conjugation [2] in **1** was considered, by introduction of a β-spiro resonance integral, equal to 0.4 eV. Spiro-conjugation was assumed to be negligible in the case of **2**, but the *Walsh* orbital system of the four-membered ring [23] was introduced into the PPP formalism, to allow 'through bond' interaction [1]. The cyclobutane *Walsh* orbitals are represented in a basis of eight p atomic orbitals, as indicated in *Figure 1*. The *Walsh* orbitals are allowed to conjugate with the π-systems of the bridging biphenyl moieties in **2**. The corresponding resonance integral $\beta_{\pi W}$, involving a pπ-orbital and a 'tangentially' oriented cyclobutane p-orbital, is chosen such that the spectral properties of simple systems like tricyclo[3.3.0.$0^{2,6}$]octa-3,7-diene, tricyclo-[3.3.0.$0^{2,6}$]octa-3-ene [24], and bicyclo[4.1.1]octa-2,4-diene [25] are well-described by calculations within the model [26] ($\beta_{\pi W}$ = 1.5 eV).

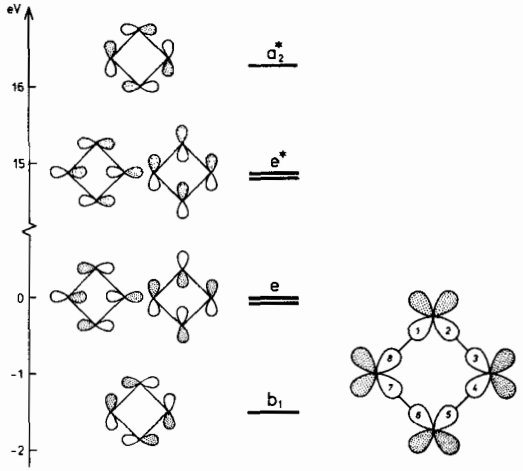

Fig. 1. Walsh *orbital system of cyclobutane as predicted by the PPP-type model.* Definition and numbering of the basis orbitals is indicated to the right. The interaction terms of the basis (right) are $\Delta I = 2.0$ eV (relative to the standard PPP value set equal to zero); $\beta_\sigma = \beta_{18} = \beta_{23} = \beta_{45} = \beta_{67} = -5.5$ eV; $\beta_\pi = \beta_{14} = \beta_{27} = \beta_{36} = \beta_{58} = -0.75$ eV. Electron repulsion as usual, with added one centre, off-diagonal $\gamma = 10.84$ eV.

CNDO/S calculations were performed using a modified version [27] of the computer program published by *Baumann* [28]. Input geometries were estimated from the results of MNDO [29] calculations with partial geometry optimization; D_{2d}-symmetry was assumed for **1** and **2**, C_{2v} for **3**. The calculated transitions indicated in *Table 2* were obtained with inclusion of 64 singly excited configurations in the case of **1** and **2**, and 16 in the case of **3**, as in the PPP calculation.

4. Photoelectron Spectra. – The PE spectrum of **2** is shown in *Figure 2;* PE spectra of **1** and **3** have been previously published [5–7]. The measured ionization energies are given in *Table 1* together with the calculated energies. The spectra

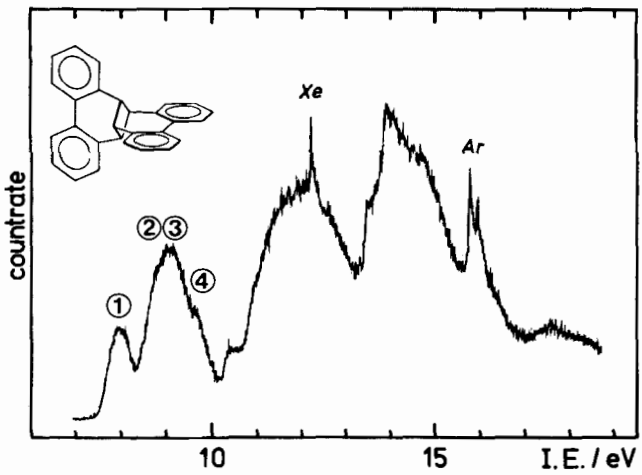

Fig. 2. *He(Iα) gas-phase photoelectron spectrum of the phenanthrene dimer* **2**

of **1** and **3** exhibit well-resolved sharp π-bands in the low-energy region [5–7], but the spectrum of **2** is poorly resolved, with broad overlapping features. Probably **2** is not a rigid molecule, as suggested by the inspection of molecular models. Also, as mentioned in *Section 2*, the spectrum of **2** may be contaminated by the presence of pyrolysis products.

The calculated PPP orbital energy level diagram is shown in *Figure 3*. The theoretical energies correlate satisfactorily with the PE data (*Koopmans'* theorem

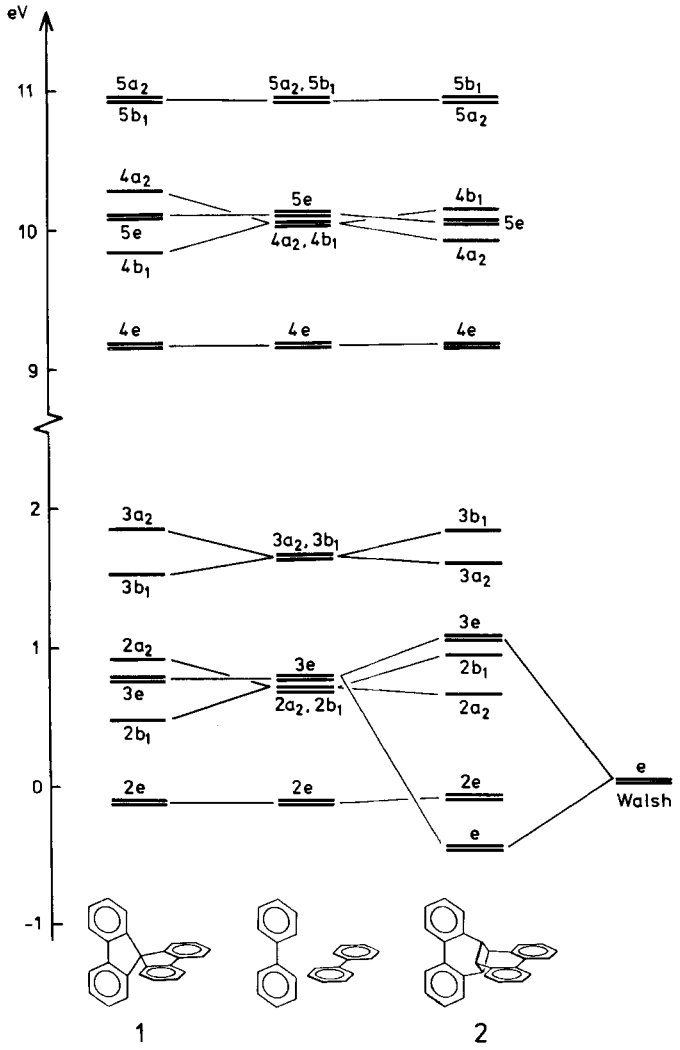

Fig. 3. *Orbital interaction diagram calculated by the PPP model, illustrating the influence of spiro conjugation in the case of* **1** *and 'through bond' interaction* via *cyclobutane* Walsh *orbitals in the case of* **2**. The highest occupied *Walsh* orbital level of cyclobutane is indicated to the right (see *Fig. 1*).

Table 1. *Measured Photoelectron Band Maxima* (or shoulders) I_J *and Calculated Orbital Energies* ε_J (eV)

Compound	Band	I_J	Orbital assignment[a])	Calculated CNDO[b])	Calculated PPP[c])
1[d])	①	7.7	$3a_2$	7.52	7.67
	②	8.0	$3b_1$	7.86	8.01
	③	8.7	3e	8.35	8.85
			$2a_2$	8.41	8.69
	④	9.4	$2b_1$	9.15	9.17
	⑤	9.9	2e	9.64	9.81
2	①	7.9	$3b_1$	7.50	7.68
			$3a_2$	7.85	7.92
	②	(8.7)	3e	8.33	8.52
	③	9.0	$2b_1$	8.33	8.65
			$2a_2$	8.74	8.96
	④	(9.6)	2e	9.57	9.77
3[e])	①	7.91	$3a_2$	7.70	7.87
	②	8.77	$4b_2$	8.40	8.85
	③	9.09	$2a_2$	8.69	8.89
	④	9.84	$3b_2$	9.61	9.81

[a]) For simplicity, the numbering refers to π-orbitals only. [b]) $-\varepsilon_J$. [c]) $-1.1\varepsilon_J + 9.7$. [d]) PE data from [7]. [e]) PE data from [6].

[30]), allowing a detailed orbital assignment of individual PE peaks for **1** and **3**, see *Table 1*. The close agreement between calculated and observed trends, including relative band intensities [7], indicates that spiro-conjugation in **1** is well-represented within the simple model. In the case of **2**, the computed energies are reasonably consistent with the observed spectrum, but the poor spectral resolution prevents a closer analysis.

5. Polarized Absorption Spectra. – 5.1. *Observed Spectra.* The reduced polarized absorption curves of **3**, **1** and **2** are shown in *Figure 4, 5* and *6*, respectively. Compared with the corresponding room-temperature spectra, a higher degree of linear dichroism (LD) and a significantly improved resolution is obtained by the low-temperature technique. This is particularly marked for **3** and **1** and is demonstrated by comparison with the curves determined at room temperature by *Sagiv et al.* [11].

In the case of **3**, the reduction factor $d_\perp^\circ$ [17] was determined from the assumption that the sharp vibronic peaks in the 33000–40000 cm^{-1} region are long-axis polarized, leading to $d_\perp^\circ = 0.25$. Using the terminology of *Eggers et al.* [17], this value corresponds to the orientation factor $K_1 = 1/(2\,d_\perp^\circ + 1) = 0.67$. The reduction factor $d_\parallel^\circ$ and the orientation factor $K_2 = d_\parallel^\circ/(2 + d_\parallel^\circ)$ cannot be determined directly from the LD spectrum because of the absence of a suitable short-axis polarized peak. Assuming that $K_1 = 0.67$ and considering a point (K_1, K_2) inside the orientation triangle [18] [19], we have $0.17 \leq K_2 \leq 0.33$. The lower limit corresponds to the cylindrical rod-like orientation distribution, which was assumed *a priori* by *Sagiv et al.* [11]. The curves in *Figure 4* were produced under the assumption that $(K_1, K_2) = (0.67, 0.20)$, corresponding to $(d_\perp^\circ, d_\parallel^\circ) = (0.25, 0.50)$; however, the results do not depend critically on the assumptions made.

As expected, **1** is much less efficiently oriented than **3**. In this case, $d_{\parallel}^{\circ}$ was determined under the assumption that the peaks close to 36000 and 39000 cm^{-1} are polarized perpendicularly to the long axis, leading to $d_{\parallel}^{\circ} = 0.82$ and $K_2 = 0.29$. $d_{\perp}^{\circ}$ (or K_1) cannot be determined independently, but in view of the high symmetry

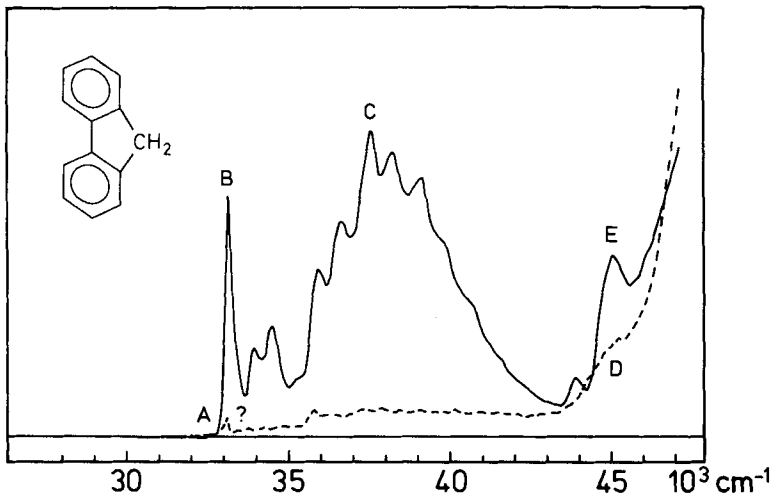

Fig. 4. *Polarized absorption spectrum of fluorene* (**3**) *in stretched polyethylene at 77 K.* The figure shows the reduced absorption curves, indicating long-axis polarized absorption $A_1 = E_{\parallel} - 0.50\ E_{\perp}$ (full line) and short-axis polarized absorption $A_2 = 1.67\ [E_{\perp} - 0.25\ E_{\parallel}]$ (dashed line), where $E_{\parallel}$ and $E_{\perp}$ are the absorption curves measured with the stretching direction parallel and perpendicular to the plane of the linearly polarized light.

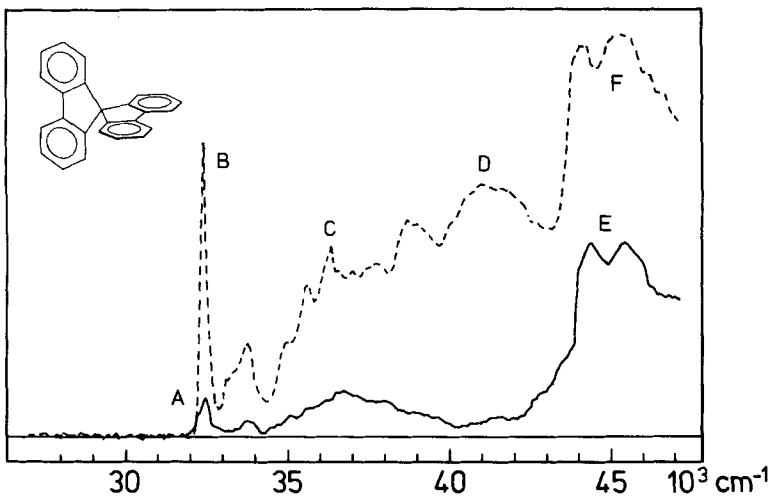

Fig. 5. *Polarized absorption spectrum of 9,9'-spirobifluorene* (**1**) *in stretched polyethylene at 77 K.* The curves indicate long-axis polarized absorption $A_1 = E_{\parallel} - 0.82\ E_{\perp}$ (full line) and short-axis polarized absorption $A_{2,3} = 1.17\ [E_{\perp} - 0.70\ E_{\parallel}]$ (dashed line); see legend to *Fig. 4.*

of the molecule (D_{2d}) and assuming that the preferred orientation axis coincides with the symmetry axis [11], the orientation of **1** can be considered to be of the cylindrical limiting-type characterized by $K_1 = 1\text{-}2\,K_2$ [17–19]. This assumption leads to $K_1 = 0.42$ and $d_\perp^\circ = 0.70$. The resulting curves in *Figure 5* are consistent with those published by *Sagiv et al.* [11].

Although **2** seems to allign even less readily than **1**, this molecule presents a more favorable case for the stepwise reduction procedure since both reduction factors can be estimated independently from the LD curves. The unreduced observed spectrum as well as the two families of reduced curves are shown in *Figure 7*. Under the assumption that the two peaks close to 42400 and 43500 cm^{-1} are long-axis polarized and the peaks close to 34300, 35700, 39000 and 40500 cm^{-1} are short-axis polarized, the linear combinations defined by $(d_\perp^\circ, d_\parallel^\circ) = (0.80, 0.85)$ can be selected with a fair degree of accuracy. The corresponding orientation factors $(K_1, K_2) = (0.38, 0.30)$ indicate within the experimental error a point on the line $K_1 = 1\text{-}2\,K_2$ describing cylindrical orientation distributions, but very close to the 'left corner' of the orientation triangle, $(K_1, K_2) = (\frac{1}{3}, \frac{1}{3})$, which corresponds to the case of completely random orientation. This result is nicely consistent with what would be predicted from the near-tetrahedral shape and symmetry of **2**. The consistency is very satisfactory and supports the philosophy behind the evaluation of stretched sheet spectra [17–19].

Inspection of the reduced polarized spectra in *Figure 4–6* indicates obvious similarities in the low-energy region (30000–38000 cm^{-1}), but significant differences at higher energies; note that long-axis (short-axis) polarized absorption in **3** corresponds to short-axis (long-axis) polarized absorption in **1** and **2**. The bands

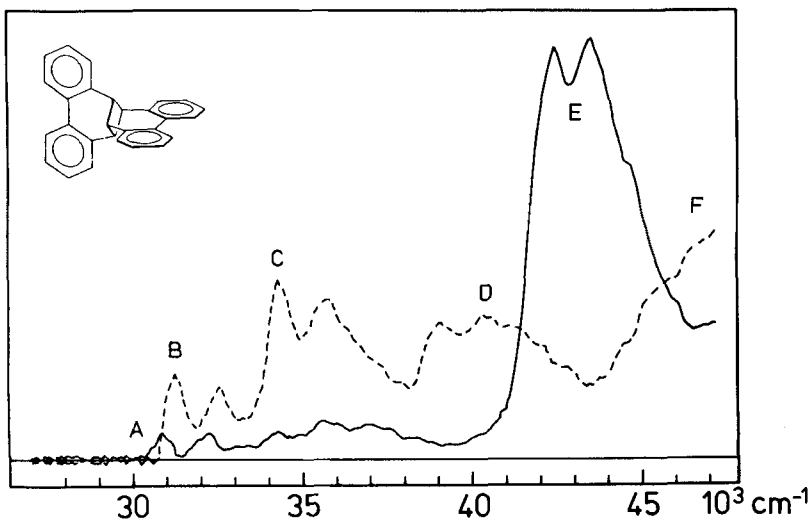

Fig. 6. *Polarized absorption spectrum of the phenanthrene dimer* **2** *in stretched polyethylene at 77 K.* The curves indicate long-axis polarized absorption $A_1 = E_\parallel - 0.85\,E_\perp$ (full line) and short-axis polarized absorption $A_{2,3} = 1.10\,[E_\perp - 0.80\,E_\parallel]$ (dashed line); see legend to *Fig. 4.*

B and *C* for **3** with maxima close to 33200 and 37600 cm^{-1} thus correspond to bands *B* and *C* for **1** (32400 and 36300 cm^{-1}) and **2** (31200 and 34300 cm^{-1}). This correspondence is particularly striking in the case of **1**, clearly indicating the close

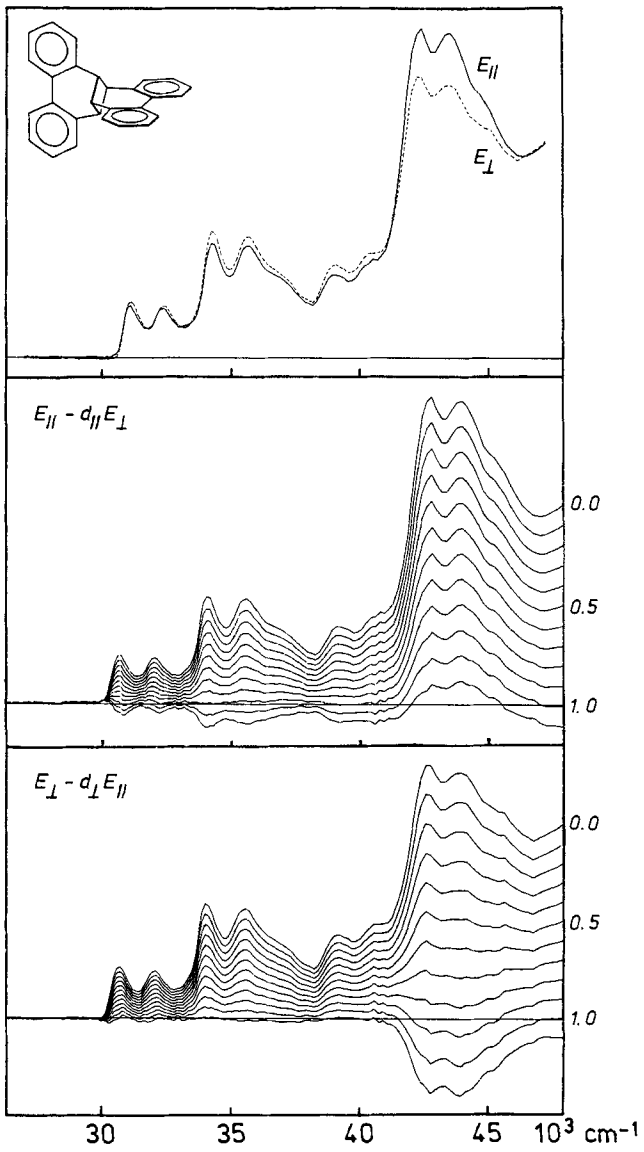

Fig. 7. *Observed, unreduced LD absorption curves* $E_{\parallel}$ *and* $E_{\perp}$ *for* **2**, *measured at 77 K in stretched polyethylene with the stretching direction parallel and perpendicular to the plane of the linearly polarized light* (top). *Families of reduced absorption curves* $E_{\parallel} - d_{\parallel}\ E_{\perp}$ *and* $E_{\perp} - d_{\perp}\ E_{\parallel}$ *according to the stepwise reduction procedure* [17] (middle and bottom).

relationship between **3** and **1**. The relative intensity of band *C*, however, is significantly reduced when passing from **3** to **1**.

Below the first intense peak *B* weaker differently polarized absorption *A* is observed in all three cases. In the case of **3** this structure close to 33100 cm^{-1} is extremely weak and could easily be an artifact of the reduction procedure; it is well-known that sharp peaks (like *B*) are frequently associated with small wiggles in the curves corresponding to differently polarized absorption in the reduced spectra [16–19]. *Tanizaki et al.* [9] assigned an s-shaped structure close to 32600 cm^{-1} (f=0.0001) in their LD spectrum of fluorene in stretched polyvinyl alcohol to an individual electronic transition. In view of the problem indicated above, we consider this assignment questionable. On the other hand, in the case of **1** and **2**, the corresponding peaks *A* close to 32400 and 30800 cm^{-1}, respectively, are prominent and cannot be explained as an artifact. In the case of **1**, the peaks *A* and *B* are degenerate within experimental resolution, but in the case of **2**, peak *A* is clearly situated at lower energy than *B;* this excludes the possibility that the absorption *A* is part of the vibronic structure of band *B* (assigning the peak labeled *B* as the purely short-axis polarized 0–0 component of this band). The peak labeled *A* in the spectra of **1** and **2** must be assigned to the onset of an individual long-axis-polarized electronic transition. Part of the long-axis polarized absorption observed below 40000 cm^{-1} probably belongs to this band, overlapping long-axis-polarized vibronic components of the bands *B* and *C* (involving non-totally symmetric vibrations). *Sagiv et al.* [11] assigned an additional long-axis polarized electronic transition close to 37000 cm^{-1} in the case of **1**; however, this assignment is neither supported by the recent results of *Palmieri & Samori* [12], nor by the results of the ensuing analysis.

In the region above 38000 cm^{-1}, the spectra of **1**, **2** and **3** show striking differences. Most significantly, the spectra of **1** and **2** exhibit a strong band *D* with maximum close to 41000 cm^{-1} which has no obvious counterpart in the spectrum of **3**. Moreover, in the case of **2** the high-energy region is dominated by a very strong long-axis polarized band *E* with maxima close to 42400 and 43500 cm^{-1}; the corresponding region of the spectrum of **1** is dominated by short-axis polarized absorption, overlapping a less intense long-axis polarized band. In the following section we investigate the origin of these differences by comparison with the results of model calculations.

5.2. *Comparison with Theory.* Biphenyl and fluorene **3** have been the subject of numerous theoretical investigations and the nature of the excited singlet states in the near-UV seems well-understood (see, *e.g.*, [3] [4] [8] [9] [11] [31–34] and literature cited there).

Transitions calculated in the PPP-CI approximation for planar D_{2h}-biphenyl are indicated in *Table 2* and shown diagrammatically in *Figure 8c*. Four transitions below 50000 cm^{-1} are predicted to be forbidden, either by the spatial or by the alternant pairing or 'plus-minus' symmetry [33] which is contained in the PPP model. In the case of **3**, both kinds of symmetry are perturbed and the corresponding transitions gain intensity. Three transitions to $^1A_\uparrow$, $^1B_\uparrow$ and $^1B_\downarrow$ states are predicted in the low-energy region; the $^1A_\uparrow$ and $^1B_\uparrow$ transitions are near-degenerate and weaker than the intense $^1B_\downarrow$ transition, which is well-described by promotion of an electron from the HOMO to the LUMO. These results are independent of the model and the extension of the CI expansion (*e.g.*, [31]). Assignment of the long-axis polarized bands *B* and *C* to the $^1B_\uparrow$ and $^1B_\downarrow$ states is straight forward. The only

Table 2. *Observed and Calculated Transitions for Fluorene* (**3**), *Spirobifluorene* (**1**), *and the Phenanthrene Dimer* **2**. The table indicates wave numbers ν in units of 1000 cm^{-1}, oscillator strengths f, and observed polarization directions p. Symmetries are given in the point groups C_{2v} (**3**) and D_{2d} (**1** and **2**); in the case of **3**, corresponding symmetries in D_{2h} are given to the right. Observed transitions for **3** and **1** in the region above 47000 cm^{-1} are estimated from the spectral curves published by *Sagiv et al.* [11].

Compound	Band	Observed			Symmetry		CNDO-CI		PPP-CI			
		ν	f	p			ν	f	ν	f		
3	*A*	33.1?		⊥	(C_{2v})	$^1A_1^-$	32.8	0.00002	35.8	–	(D_{2h})	B_{1u}^-
	B	33.2	0.05	∥		$^1B_1^-$	33.3	0.04	36.3	–		B_{2g}^-
	C	37.6	0.35	∥		$^1B_1^+$	36.3	0.29	37.4	0.88		B_{3u}^+
	D	45	0.02	⊥		$^1A_1^+$	44.2	0.00043	48.7	–		A_g^+
	E	45.0	0.05	∥		$^1B_1^+$	45.2	0.07	47.4	–		B_{2g}^+
	F	48		⊥		$^1A_1^+$	46.6	0.43	49.7	1.02		B_{1u}^+
	G	49		∥		$^1B_1^+$	46.6	0.59	50.8	1.28		B_{3u}^+
1	*A*	32.4	0.01	∥	(D_{2d})	$^1B_2^-$	32.7	0.00008	35.5	0.0035		
	B	32.4	0.1	⊥		$^1E^-$	32.7	0.11	35.8	0.12		
						$^1A_1^-$	32.7	–	35.8	–		
	C	36.3	0.4	⊥		$^1E^+$	35.7	0.37	36.8	1.22		
	D	41.1	0.6	⊥		$^1E^-$	40.8	0.17	41.5	0.26		
	E	44.4	0.4	∥		$^1B_2^+$	41.3	0.33	45.4	0.90		
	F	45.3	0.8	⊥		^1E	43.6	0.40	48.5	0.37		
	G	48		∥		$^1B_2$	44.0	0.25	48.7	0.36		
	H	51		⊥		^1E	46.3	0.70	50.8	1.92		
	I	51		∥		$^1B_2$	47.6	0.40	50.5	0.69		
2	*A*	30.8	0.02	∥	(D_{2d})	$^1B_2^-$	33.1	0.00048	35.3	0.0044		
	B	31.2	0.07	⊥		$^1E^-$	32.9	0.054	36.0	0.40		
						$^1A_1^-$	33.2	–	35.4	–		
	C	34.3	0.4	⊥		$^1E^+$	35.6	0.50	36.5	0.98		
	D	40.5	0.4	⊥		$^1E^-$	42.3	0.11	43.4	0.16		
	E	43.5	1.2	∥		$^1B_2^+$	42.4	0.44	44.9	1.49		
						$^1B_2$	44.6	0.37	48.2	0.51		
	F	48		(⊥)		^1E	45.0	0.24	46.2	0.24		
						^1E	46.1	0.80	48.6	2.20		

complication concerns the $^1A_1^-$ state predicted as the lowest excited singlet state; the transition is predicted to be extremely weak and is not clearly observed in the experimental spectrum. The weak short-axis polarized peak *A* observed below the *B* peak could easily be assigned to the $^1A_1^-$ state; this assignment is supported by the unambigous observation of corresponding transitions for **1** and **2**. The short-axis polarized structure at 35800 cm^{-1} may belong to the $^1A_1^-$ band but the assignment is complicated by overlap with the much stronger *B* and *C* bands. The 35800 cm^{-1} structure seems to correspond to a sharp peak in the magnetic circular dichroism (MCD) spectrum [34]; the interpretation of the MCD spectrum of fluorene is not straightforward, but the spectrum is consistent with the assumption of two overlapping transitions with opposite MCD signs in the 33000–36000 cm^{-1} region.

The results of PPP-CI calculations for two mutually perpendicular biphenyls arranged as in the case of **1** and **2**, but without consideration of long-distance conjugative effects, are indicated in *Figure 8b* and *8d*, respectively. In this approximation the alternant pairing symmetry is maintained, and the point group symmetry is D_{2d}. The calculated spectra are influenced by exciton electrostatic interactions between the chromophores [3] [4]. The dipole-dipole interaction vanishes for transitions which are not polarized parallel to the symmetry axis of the dimer (the long-axis). However, even in the case of first-order exciton interaction involving

very strong long-axis polarized transitions, the effect is modest, leading to energy shifts less than 2000 cm^{-1}. This is understandable in view of the considerable distance between the centers of two non-conjugated benzene rings (*ca.* 5 Å in **1**).

The most important interaction between the chromophores is of charge-resonance type, leading to the prediction of a charge-resonance state *CR* [3,4] at relatively low energy as indicated in *Figure 8b* and *8d*. This state involves promotion of an electron from the highest occupied MO (HOMO) of one chromophore to the lowest unoccupied MO (LUMO) of the other, *i.e.*, $|1 \rightarrow -1'>$ and $|1' \rightarrow -1>$, giving rise to a doubly degenerate 'minus' state $^1E^-$. The corresponding *intra*-chromophore HOMO-LUMO transitions $|1 \rightarrow -1>$ and $|1' \rightarrow -1'>$ are strongly allowed and give rise to an $^1E^+$ state. This transition corresponds to the prominent fluorene *C* band at 37600 cm^{-1}. Transition to the $^1E^-$ charge-resonance state of the dimer is predicted to occur 4000–7000 cm^{-1} towards higher energy but is forbidden in the absence of long-distance conjugative effects and by the pairing symmetry. When spiro or 'through-bond' conjugation is introduced into the model as described in *Section 3*, the charge-resonance transition gains intensity, particularly as a result of configuration interaction with the optically allowed *intra*-chromophore HOMO-LUMO configurations. This interaction is permitted in the PPP-CI model only because of perturbation of the pairing symmetry by the long-range effects. In the case of the CNDO-CI model the pairing symmetry is only quite approximate and the charge-resonance transition is predicted to be of mixed nature and relatively intense.

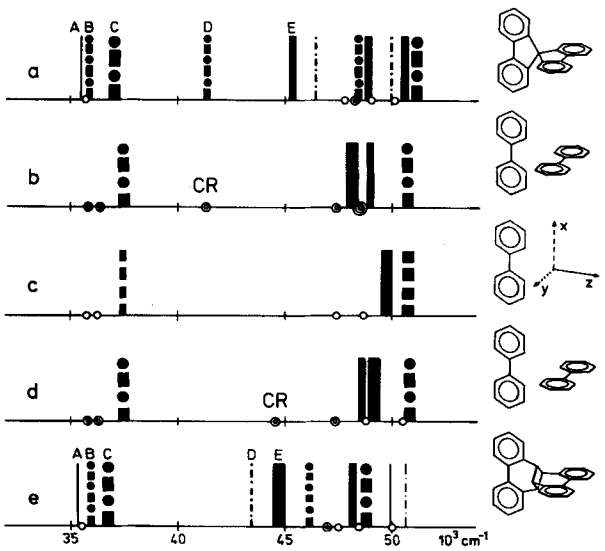

Fig. 8. *Calculated PPP-CI singlet-singlet transitions.* x-, y-, and z-polarized transitions are indicated by 'broken', 'dotted' and 'full' bars, respectively. Transitions to states of E-symmetry in the D_{2d}-species are indicated by the appropriate mixed symbolism. The thickness of the bars indicates the relative oscillator strengths, forbidden transitions are indicated by circles.

The assignment of the short-axis polarized band *D* in the spectra of **1** and **2** close to 41000 cm^{-1} now becomes straight forward. We assign this band, which has no direct counterpart in the spectrum of **3**, to the charge-resonance state discussed above, in excellent agreement with the calculated transition energy. The transition is not of pure charge-resonance type, but is predicted to borrow most of its intensity by configuration interaction; additional contributions to the considerable intensity of the observed band may be of vibronic origin. The assumption that configuration interaction is significant is supported by a consideration of the intensity shift of the *C* band when going from **3** to **1**. As in the case of the *B* transition, one would expect the intensity to increase by a factor two; however, the intensity of the *C* transition is essentially unaffected. This observation is most reasonably explained by the assumption that the intensity of the parent fluorene *C* transition is diluted in **1** as a result of configuration interaction, involving the intrinsically near-forbidden charge-transfer configurations. Vibronic interactions may further contribute to the observed trend.

It is interesting to compare with the related case of spiro[4.4]nonatetraene (**4**). This compound has a similar frontier orbital pattern as **1** (see *Fig. 3*) but the spiro-

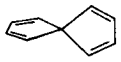

4

conjugative splitting of the two HOMO's a_2 and b_1 is much larger, amounting to 1.23 eV or 9900 cm^{-1} as estimated by PE spectroscopy [35]. This can be explained by the larger orbital amplitudes on the centers participating in the spiro-conjugation. It was pointed out by *Heilbronner et al.* [35] that for **4** the splitting in energy of the two HOMO-LUMO transitions $a_2 \rightarrow e$ and $b_1 \rightarrow e$, corresponding to the observed band maxima at 37200 and 47200 cm^{-1}, is essentially identical to the splitting of the two HOMO's. In the case of **1** and **2**, long-range conjugation is less significant and the difference in energy of the two HOMO-LUMO states is dominated by the different electron interaction terms for *intra-* and *inter*-chromophore transitions.

For **1** and **2**, the spectral region above the *D* transition is complex, involving about a dozen calculated transitions within a narrow energy range as indicated in *Figure 8a* and *8e*. The calculated results in this region are strongly affected by the perturbation of the pairing symmetry by the long-range effects, leading to essentially first-order interaction between a large number of 'plus'- and 'minus'-type configurations. For the resulting states, assignment of charge-resonance and exciton character or 'plus' and 'minus' labels seems unreasonable because of the profound mixing. Also correlation of transitions in the series **1**, **2** and **3** becomes ambigous. The calculated transitions depend primarily on configurations other than those of HOMO-LUMO type discussed above, involving the orbitals next to the frontier region. The diagram in *Figure 3* indicates rather different orbital patterns for **1** and **2** outside the frontier region, consistent with the observation of obvious spectral differences in the high-energy region.

Inspection of the calculated wave functions suggests that the remarkably increased long-axis polarized intensity in the case of **2** (*i.e.*, band E) can be explained as a result of the 'through bond' interaction. As shown in *Figure 3*, the 3e-orbital of **2** is significantly destabilized by interaction with the highest occupied *Walsh* orbitals of the four-membered ring (see *Fig. 1*), leading to increased importance of excitations involving the 3e-electrons in the near-UV region. According to the PPP-CI calculation, the strongly allowed $^1B_{\frac{1}{2}}$ state calculated close to 44000 cm^{-1} can be described as 55% $3a_2 \rightarrow 4b_1$, 12% $3e \rightarrow 4e$, and 10% $2a_2 \rightarrow 4b_1$ in the case of **1**, but as 39% $3b_1 \rightarrow 4a_2$, 31% $3e \rightarrow 4e$, and 14% $3e \rightarrow 5e$ in the case of **2**. The intensity of the transition is increased by more than 60% in the latter case. However, not unexpectedly, in this complex region the results of the CI calculation are sensitive to the model; the CNDO-CI results, which are in good agreement with the observed spectra, indicates that the intense *E* band in the case of **2** can be assigned to two overlapping strong transitions, corresponding more or less to the transitions *E* and *G* in the case of **1** (see *Table 2*).

6. Concluding Remarks. – The LD data for **1** and **2** are particularly important in that they provide a test case for the general assumptions underlying the 'orientation triangle' [18] [19]. **1** and **2** are near-spherical species of D_{2d}-symmetry and provide new points for the 'orientation triangle' close to the corner corresponding to random orientation distributions. The consistency between predicted and observed orientation characteristics for **2** is very satisfactory and supports the philosophy behind the treatment of stretched sheet spectra of *Eggers et al.* [17–19].

According to our analysis, the first three excited singlet states *A*, *B* and *C* of **1** and **2** can be described in terms of transitions localized in one biphenyl moiety, although state *C* is significantly perturbed by admixture of charge-resonance contributions. The fourth excited state *D*, however, is best described as a charge-resonance state, gaining optical intensity by long-distance conjugative effects (spiroconjugation, 'through bond' interaction), configuration interaction and probably vibronic interactions. The comparable energies and oscillator strengths of the band *D* in the spectra of **1** and **2** are consistent with the assumption that spiroconjugation in **1** plays a similar role as 'through bond' interaction *via* the four-membered ring in **2** [1]. This assumption is furthermore supported by the results of model calculations for **1** and **2**. In this connection, calculations within the PPP-CI model with representation of long-distance conjugative interactions as discussed in *Section 3* are particularly useful, allowing a detailed study of the different 'effects'.

We finally wish to emphasize that the results of this analysis are in contrast to the general assumptions of *Sagiv et al.* [11] concerning the electronic structure of **1**. These authors base their interpretation on a pure exciton model, assuming that charge-resonance contributions can be neglected in a qualitative description. In our opinion, it would have been more justified to neglect exciton interaction and consider explicitly charge-resonance effects. In particular, within a pure exciton-picture assignment of the intense *D* transition with maximum close to 41 000 cm^{-1} is problematic. *Sagiv et al.* correlate this transition with the much weaker fluorene *E* transition observed at 45 000 cm^{-1}, explaining the energy lowering as a result of spiro-conjugation and vibronic interactions. However, as discussed in this work, consideration of charge-resonance contributions leads to the prediction of an additional excited state in this energy region and a straight-forward assignment of the *D* band. On the other hand, *Sagiv et al.* assign an additional long-axis polarized transition close to 37 000 cm^{-1}, which is not consistent with our results. According to *Sagiv et al.*, this transition originates from the fluorene *D* transition

close to 45000 cm^{-1} which is shifted towards lower energies in **1** because of exciton dipole-dipole interaction. We find that a stabilization of 8000 cm^{-1} is physically unrealistic, in view of the distance between the interacting chromophores and the weakness of the fluorene *D* band ($f \approx 0.02$). The long-axis polarized absorption observed in this region can probably be assigned to vibronic components of the overlapping transitions *A*, *B* and *C*.

We are grateful to Prof. Dr. *D. Hellwinkel* for kind gifts of samples of **1** and **3**, to Prof. Dr. *H. Bock* for measuring a preliminary PE spectrum of **2**, and to Dipl.-Chem. *H.-J. Enders* for part of the synthesis of **2**. This work was supported by the *Deutsche Forschungsgemeinschaft*, the *Fonds der Chemischen Industrie* and the *BASF Aktiengesellschaft* (Ludwigshafen).

REFERENCES

[1] *P. Bischof, R. Gleiter & R. Haider,* Angew. Chem. *89*, 122 (1977); Angew. Chem. Int. Ed. Engl. *16*, 110 (1977); J. Am. Chem. Soc. *100*, 1036 (1978).
[2] *H.E. Simmons & T. Fukunaga,* J. Am. Chem. Soc. *89*, 5208 (1967); *R. Hoffmann, A. Imamura & G.D. Zeiss,* J. Am. Chem. Soc. *89*, 5215 (1967); *H. Dürr & R. Gleiter,* Angew. Chem. *90*, 591 (1978); Angew. Chem. Int. Ed. Engl. *17*, 559 (1978).
[3] *J.N. Murrell,* 'The Theory of the Electronic Spectra of Organic Molecules', Methuen 1963.
[4] *H. Suzuki,* 'Electronic Absorption Spectra and Geometry of Organic Molecules', Academic Press 1967.
[5] *J.P. Maier & D.W. Turner,* Discus. Faraday Soc. *54*, 149 (1972).
[6] *B. Ruščić, B. Kovač & L. Klasinc,* Z. Naturforsch. A*33*, 1006 (1978); *L. Klasinc,* Pure Appl. Chem. *52*, 1509 (1980).
[7] *A. Schweig, U. Weidner, D. Hellwinkel & W. Krapp,* Angew. Chem. *85*, 360 (1973); Angew. Chem. Int. Ed. Engl. *12*, 310 (1973).
[8] *G. Hohlneicher, F. Dörr, N. Mika & S. Schneider,* Ber. Bunsenges. Phys. Chem. *72*, 1144 (1968); *B. Dick, H. Gonska, G. Hohlneicher,* Ber. Bunsenges. Phys. Chem. *85*, 746 (1981).
[9] *T. Hoshi, H. Inove, J. Shiraishi & Y. Tanizaki,* Bull. Chem. Soc. Jpn. *44*, 1743 (1970); *T. Yoshinaga, H. Hiratsuka & Y. Tanizaki,* ibid. *51*, 996 (1978).
[10] *H. Labhart, E.R. Pantke & K. Seibold,* Helv. Chim. Acta *55*, 658 (1972).
[11] *J. Sagiv, A. Yogev & Y. Mazur,* J. Am. Chem. Soc. *99*, 6861 (1977).
[12] *P. Palmieri & B. Samori,* J. Am. Chem. Soc. *103*, 6818 (1981).
[13] *G. Wittig & G. Skipka,* Liebigs. Ann. Chem. *1975*, 1157.
[14] *H.J. Enders,* Master Thesis, Technische Hochschule Darmstadt 1980; *R. Haider,* Ph D Thesis, Universität Heidelberg 1982.
[15] *J. Spanget-Larsen, R. Gleiter, R. Haider & E.W. Thulstrup,* Mol. Phys. *34*, 1049 (1977).
[16] *E.W. Thulstrup, J. Spanget-Larsen & R. Gleiter,* Mol. Phys. *37*, 1381 (1979).
[17] *E.W. Thulstrup, J. Michl & J. Eggers,* J. Phys. Chem. *74*, 3868 (1970); *J. Michl, E.W. Thulstrup & J. Eggers,* ibid. *74*, 3878 (1970).
[18] *E.W. Thulstrup & J. Michl,* J. Am. Chem. Soc. *98*, 4533 (1976); ibid. *104*, 5594 (1982); J. Phys. Chem. *84*, 82 (1980).
[19] *E.W. Thulstrup,* 'Aspects of the Linear and Magnetic Circular Dichroism of Planar Organic Molecules', Springer-Verlag, Heidelberg 1980.
[20] *R. Pariser & R.G. Parr,* J. Chem. Phys. *21*, 466 (1953); *J.A. Pople,* Trans. Faraday Soc. *49*, 1375 (1953).
[21] *H.H. Jaffé,* Acc. Chem. Res. *2*, 136 (1969) and references given therein.
[22] *N. Mataga & K. Nishimoto,* Z. Phys. Chem. *13*, 140 (1957).
[23] *R. Hoffmann & R.B. Davidson,* J. Am. Chem. Soc. *93*, 5699 (1971).
[24] *R. Gleiter & T. Kobayashi,* Helv. Chim. Acta *54*, 1081 (1971).
[25] *R. Gleiter, P. Bischof, W.E. Volz & L.A. Paquette,* J. Am. Chem. Soc. *99*, 8 (1977).

[26] *J. Spanget-Larsen,* unpublished results.
[27] *J. Spanget-Larsen & R. Gleiter,* Helv. Chim. Acta *61*, 2999 (1978).
[28] *H. Baumann,* QCPE *10*, 333 (1977).
[29] *M.J.S. Dewar & W. Thiel,* J. Am. Chem. Soc. *99*, 4899 (1977); *P. Bischof & G. Friedrich*, J. Comp. Chem. *3*, 486 (1982).
[30] *T. Koopmans,* Physica *1*, 104 (1934).
[31] *J. Baraldi, M.C. Bruni & F Momicchioli,* Chem. Phys. *33*, 393 (1978).
[32] *F.T. Marchese, D.J. Seliskar & H.H. Jaffé,* J. Chem. Phys. *72*, 4194 (1980).
[33] *J.A. Pople,* Proc. Phys. Soc. A*68*, 81 (1955); *R. Pariser,* J. Chem. Phys. *24*, 250 (1956).
[34] *A. Tajiri, H. Uchimura & M. Hatano*, Chem. Letters *1975*, 1021.
[35] *C. Batich, E. Heilbronner, E. Rommel, M.F. Semmelhack & J.S. Foos,* J. Am. Chem. Soc. *96*, 7662 (1974).